Dalton Transactions

PAPER

View Article Online
View Journal | View Issue

Cite this: *Dalton Trans.*, 2015, **44**, 10708

An unusual high-spin ground state of Co^{3+} in octahedral coordination in brownmillerite-type cobalt oxide

S. Ya. Istomin,*[a] O. A. Tyablikov,[a] S. M. Kazakov,[a] E. V. Antipov,[a] A. I. Kurbakov,[b,c] A. A. Tsirlin,[d,e] N. Hollmann,[e] Y. Y. Chin,[f] H.-J. Lin,[f] C. T. Chen,[f] A. Tanaka,[g] L. H. Tjeng[e] and Z. Hu[e]

Received 30th November 2014,
Accepted 29th January 2015

DOI: 10.1039/c4dt03670k

www.rsc.org/dalton

The crystal and magnetic structures of brownmillerite-like $Sr_2Co_{1.2}Ga_{0.8}O_5$ with a stable Co^{3+} oxidation state at both octahedral and tetrahedral sites are refined using neutron powder diffraction data collected at 2 K (S.G. *Icmm*, a = 5.6148(6) Å, b = 15.702(2) Å, c = 5.4543(6) Å; R_{wp} = 0.0339, R_p = 0.0443, χ^2 = 0.775). The very large tetragonal distortion of CoO_6 octahedra (1.9591(4) Å for Co–O_{eq} and 2.257(6) Å for Co–O_{ax}) could be beneficial for the stabilization of the long-sought intermediate-spin state of Co^{3+} in perovskite-type oxides. However, the large magnetic moment of octahedral Co^{3+} (3.82(7)μ_B) indicates the conventional high-spin state of Co^{3+} ions, which is further supported by the results of a combined theoretical and experimental soft X-ray absorption spectroscopy study at the Co-$L_{2,3}$ edges on $Sr_2Co_{1.2}Ga_{0.8}O_5$. A high-spin ground state of Co^{3+} in $Sr_2Co_{1.2}Ga_{0.8}O_5$ resulted in much lower in comparison with a $LaCoO_3$ linear thermal expansion coefficient of 13.1 ppm K^{-1} (298–1073 K) determined from high-temperature X-ray powder diffraction data collected in air.

Introduction

Trivalent cobalt ($3d^6$) adopts different spin states: low-spin, LS ($t_{2g}^6e_g^0$, S = 0), high-spin, HS ($t_{2g}^4e_g^2$, S = 2), and, possibly, intermediate-spin, IS ($t_{2g}^5e_g^1$, S = 1). The particular spin state of Co^{3+} ions depends on their coordination number, strength of the crystal field, and even on temperature. For six-fold-coordinated Co^{3+} in three-dimensional structures, the LS ground state was observed in $LaCoO_3$ at low temperatures[1] and in $EuCoO_3$.[2] In layered cobaltates with octahedrally coordinated cobalt like in $LaSrCoO_4$, the coexistence of HS and LS states has been proposed.[3,4] In the case of $Ca_3Co_2O_6$, two Co^{3+} sites are notably different being LS and HS in the CoO_6 octahedra and trigonal prisms, respectively.[5] Coordination numbers below 6 will generally stabilize the HS-Co^{3+}, as in Sr_2CoO_3Cl[2] and $GdBaCo_2O_{5.5}$,[6] where CoO_5 tetragonal pyramids are present and in $YBaCo_4O_7$ with Co^{3+} is tetrahedra.[7]

In contrast to multiple examples of both LS- and HS-Co^{3+}, the IS state of Co^{3+} remains elusive. Despite multiple conjectures in the recent literature,[8–15] no conclusive evidence of the presence of IS-Co^{3+} in oxides has been reported to date. From the general crystal-field arguments, the stabilization of the IS state in the octahedral coordination requires that the degeneracy of two e_g levels is removed by a suitable distortion of the octahedral local environment, and one of the e_g levels is pushed down in energy. This kind of distortion can be found in structures with axially elongated CoO_6 octahedra.[16] Alternatively, the IS state may be formed at high temperatures following electron delocalization in the e_g bands.[17]

Spin states of Co^{3+} and relevant transformations are among basic microscopic features of Co-based oxide materials. Many of these compounds enjoy simultaneous presence of electronic and oxide-ion conductivity at high temperatures, which renders them promising materials for high-temperature electrochemical devices like cathodes for intermediate temperature solid oxide fuel cells (IT-SOFC) or dense ceramic membranes to separate oxygen from gas mixtures. One of the main drawbacks of cobaltates is their high thermal expansion coefficient (TEC) exceeding 20 ppm K^{-1} for $LaCoO_3$.[18,19] This large thermal expansion does not fit with that of solid electro-

[a]*MSU-MPG Partner Group and the Chemistry Department, Lomonosov Moscow State University, Russia. E-mail: istomin@icr.chem.msu.ru; Fax: +7 495 9394788; Tel: +7 495 9394788*
[b]*Petersburg Nuclear Physics Institute, NRC Kurchatov Institute, Gatchina, Russia*
[c]*Faculty of Physics, Saint-Petersburg State University, Petrodvorets, Ulyanovskaya str., 1, Saint-Petersburg, 198504, Russia*
[d]*National Institute of Chemical Physics and Biophysics, Akadeemia tee 23, 10628 Tallinn, Estonia*
[e]*Max Planck Institute for Chemical Physics of Solids, Noethnizer Straße 40, DE-01187 Dresden, Germany*
[f]*National Synchrotron Radiation Research Center, 101 Hsin-Ann Road, Hsinchu 30077, Taiwan*
[g]*Department of Quantum Matter, ADSM, Hiroshima University, Higashi-Hiroshima 739-8530, Japan*

lytes in SOFC, like $Zr_{1-x}Y_xO_{2-x/2}$ (YSZ) and $Ce_{1-x}Gd_xO_{2-x/2}$ (GDC) featuring TECs of 10.5 ppm K^{-1} and 12.5 ppm K^{-1}, respectively. High TECs for cobalt-related perovskites are due to the temperature activated LS–HS transitions of Co^{3+}.[19,20] Therefore, the knowledge of the spin state of Co^{3+} and the understanding of underlying microscopic parameters are crucial for the design of the materials operating in a wide temperature range.

Here, we focus on Co-based brownmillerite compounds. The brownmillerite $A_2B_2O_5$ structure is a derivative of the perovskite aristotype, where ordering of the oxygen vacancies results in alternating oxygen-rich layers of BO_6 octahedra and oxygen-deficient layers of BO_4 tetrahedra (Fig. 1). The BO_6 octahedra turn out to be axially elongated. Their equatorial oxygen atoms link two octahedra, whereas axial oxygens are shared between an octahedron and a tetrahedron. The tetrahedrally coordinated Co^{3+} imposes a higher valence on oxygen in the axial position, hence the separation of this oxygen from the octahedrally coordinated B-cation must be increased, as in Ca_2FeAlO_5, where the equatorial and axial (Fe/Al)–O distances are 1.942–1.954 Å and 2.217 Å, respectively.[21] This type of local environment would be ideal for stabilizing the putative IS-Co^{3+}.

Co^{3+}-containing brownmillerites are quite rare. Known examples include $Sr_2Co_2O_5$, which is stable above ~900 °C in air,[22–26] $Sr_2Co_{2-x}Ga_xO_5$ ($0.3 \le x \le 0.8$),[27] $Sr_2Co_{2-x}Al_xO_5$ ($0.3 \le x \le 0.5$),[28] $Ca_2Co_{1.6}Ga_{0.4}O_5$[29] and $Ca_2Co_{2-x}Al_xO_5$ ($x \approx 0:75$).[30] The spin state of Co^{3+} in these compounds has never been probed by a direct spectroscopic experiment. Indirect information can be obtained from the magnetic moments measured by neutron diffraction. However, previous neutron experiments were mostly performed at room temperature and, therefore, revealed magnetic moments reduced by thermal fluctuations.[27,29] In addition, the interpretation of the reduced moment in a system where Co^{3+} is mixed with non-magnetic Ga^{3+} and Al^{3+} may not be straightforward. With both uncertainties eliminated in $Sr_2Co_2O_5$, the neutron results remain puzzling because they reveal the magnetic moment of $3.0\mu_B$ on Co^{3+} ions,[24] which is lower than $4\mu_B$ expected for the HS state. On the other hand, density-functional calculations[24,31] and the low TEC value[24,26] indicate the HS state of Co^{3+} in this compound. Recently $La_xSr_{2-x}CoGaO_{5+y}$ compounds with the brownmillerite structure and cobalt in a mixed oxidation state between +2 and +3 were prepared.[32] From magnetic susceptibility data it was concluded that HS-Co^{3+} is present in Sr-rich compositions, while LS-Co^{3+} is observed in La-rich ones.

In the following section, we explore the spin state of Co^{3+} in $Sr_2Co_{1.2}Ga_{0.8}O_5$, which is stable in a wide temperature range in contrast to the parent compound $Sr_2Co_2O_5$.[27] We used low-temperature neutron diffraction and soft X-ray absorption spectroscopy as well as cluster calculations and density-functional band-structure calculations in order to identify the spin state of Co^{3+} ions and understand its microscopic origin.

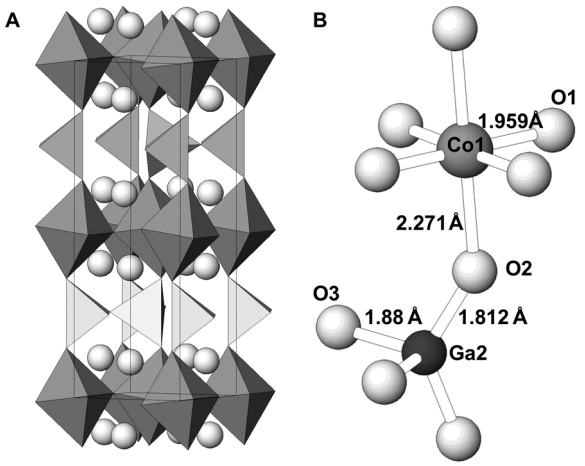

Fig. 1 The crystal structure of brownmillerite-like cobaltate $Sr_2Co_{1.2}Ga_{0.8}O_5$ (A).[27] Octahedral sites are mainly occupied by Co^{3+}, tetrahedral sites by Ga^{3+} cations. Interatomic distances in octahedron and tetrahedron (B) from ref. 27 are given in order to stress large distortion of CoO_6 octahedra in the structure.

Experimental section

A sample of $Sr_2Co_{1.2}Ga_{0.8}O_5$ was prepared by the procedure described in ref. 26. The neutron powder diffraction data at T = 2 K were collected in LLB-Saclay (France) by using a 7-sectional, 70-counter G4.2 high-resolution diffractometer (λ = 2.3433 Å from 3° to 143°). The refinement of the nuclear and magnetic structures was done using the GSAS suite of programs.[33]

High-temperature X-ray powder diffraction (HT XRPD) data were collected in air at 298–973 K using a Bruker D8-Advance diffractometer ($CuK_{\alpha 1}$ radiation, LynxEye PSD) in reflection mode equipped with a high-temperature camera XRK-900 (Anton Paar). Unit cell parameters of $Sr_2Co_{1.2}Ga_{0.8}O_5$ at high temperatures were obtained from the refinement of their crystal structures by the Rietveld method using the TOPAS-3 program package.

The soft X-ray absorption spectroscopy (XAS) was performed at the BL11A beamlines of the National Synchrotron Radiation Research Centre (NSRRC) in Taiwan. The Co-$L_{2,3}$ spectra were recorded in the total electron yield (TEY) mode with the photon energy resolution of 0.3 eV. Clean sample surfaces were obtained by cutting pellets *in situ* just before collecting the data in an ultrahigh vacuum chamber with the pressure in the range of 10^{-10} mbar. A CoO single crystal was also measured simultaneously to serve as an absolute energy calibration.

The band structure for ordered structural models of $Sr_2Co_{1.2}Ga_{0.8}O_5$ was calculated using the FPLO code[34] with the Perdew–Wang flavour of the exchange–correlation potential.[35] Orbital energies were extracted by fitting relevant bands with Wannier functions based on Co 3d orbitals.

Results and discussion

The refinement of the crystal structure of $Sr_2Co_{1.2}Ga_{0.8}O_5$ using NPD data collected at T = 2 K was performed using a

Table 1 Structural parameters for $Sr_2Co_{1.2}Ga_{0.8}O_5$ based on the refinement of NPD data at 2 K (S.G. *Icmm*, a = 5.6148(6) Å, b = 15.702(2) Å, c = 5.4543(6) Å; R_{wp} = 0.0339, R_p = 0.0443, χ^2 = 0.775)

Site	x	y	z	g (Co/Ga)	U_{iso} 100 (Å^2)
Sr	0.012(1)	0.1111(3)	0.5	1.0	1.2(2)
M1[a]	0.0	0.0	0.0	0.88/0.12[b]	0.3(3)
M2[a]	−0.073(2)	0.25	0.037(3)	0.21/0.29[b]	0.3(3)
O1	0.25	−0.0058(5)	0.25	1.0	1.8(2)
O2	0.049(1)	0.1426(4)	0.0	1.0	1.5(2)
O3	0.862(2)	0.25	0.625(2)	0.5	2.8(6)

[a] Magnetic moments are M1 = 3.36(7)μ_B and M2 = 1.7μ_B (fixed). [b] Refined chemical composition of the brownmillerite phase is $Sr_2Co_{1.3}Ga_{0.7}O_5$.[27]

Table 2 Selected interatomic distances (in Å) for $Sr_2Co_{1.2}Ga_{0.8}O_5$ (T = 2 K)

O1–M1:	(×4)	1.9591(4)
O2–M1:	(×2)	2.257(6)
O2–M2:	(×2)	1.829(8)
O3–M2:	—	1.88(2)
	—	1.85(1)
Sr–O1:	(×2)	2.600(7)
	(×2)	2.647(7)
Sr–O2:	—	2.513(8)
	(×2)	2.78(1)
Sr–O3:	(×2)	2.438(9)

structure model (space group *Icmm*) that assumes disordered orientation of tetrahedral chains in oxygen-deficient layers.[27] The magnetic structure was refined in the model corresponding to the G-type arrangement of magnetic moments of Co^{3+}, with moments directed along the c-axis of the brownmillerite structure (magnetic space group *Icm′m′*). Occupancies of Co/Ga positions were measured from the refinement of the crystal structure of $Sr_2Co_{1.2}Ga_{0.8}O_5$ at room temperature[27] and were not refined (the same sample was used for both room-temperature refinement in ref. 27 and the present low-temperature experiment). It should be noted that the refined composition of the brownmillerite phase in the $Sr_2Co_{1.2}Ga_{0.8}O_5$ sample in ref. 27 was slightly different from the nominal one and corresponds to the chemical formula $Sr_2Co_{1.3}Ga_{0.7}O_5$. The final structural and refinement data are given in Table 1, selected interatomic distances are presented in Table 2, and observed, calculated and difference NPD profiles are shown in Fig. 2. Considering the static disorder of atoms in the tetrahedral layer and the presence of non-magnetic Ga^{3+} cations, during the final refinement the magnetic moment of cobalt on the M2 tetrahedral site was set at 4μ_B, as expected for HS-Co^{3+}, because at the tetrahedral site only HS-Co^{3+} can be envisaged.[10] The refined magnetic moment of cobalt on the octahedral M1 site is 3.36(7)μ_B per site. Note that the simultaneous refinement of the magnetic moments of cobalt on the octahedral M1 and tetrahedral M2 sites does not lead to the substantial deviation from this value. Therefore, the calculated magnetic moment of Co^{3+} at the octahedral site is 3.82(7)μ_B per cobalt indicating the HS state of Co^{3+} at low temperatures.

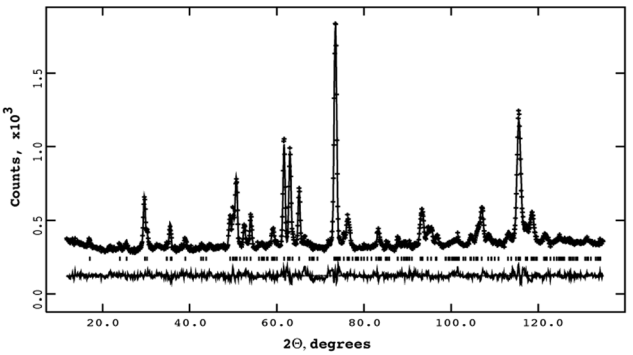

Fig. 2 Observed, calculated and difference NPD profiles for $Sr_2Co_{1.2}Ga_{0.8}O_5$ (T = 2 K).

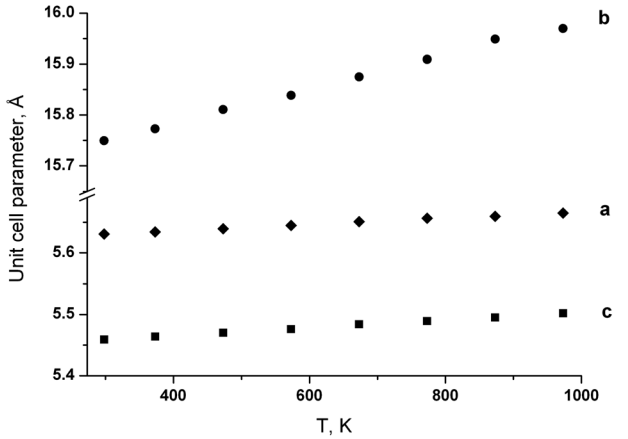

Fig. 3 Temperature variation of the unit cell parameters for $Sr_2Co_{1.2}Ga_{0.8}O_5$.

HT XRPD showed that $Sr_2Co_{1.2}Ga_{0.8}O_5$ expands linearly (Fig. 3) with TECs 9.2, 21.3 and 11.6 ppm K^{-1} for individual unit cell parameters a, b and c, respectively. The linear TEC value calculated from the temperature dependence of unit cell volume ($V^{1/3}$) is 13.1 ppm K^{-1}. This value is much lower in comparison with other perovskite-related oxides with Co^{3+}-like $LaCoO_3$. For example, $LaCoO_3$ exhibits as high TEC as 24.6 ppm K^{-1} (calculated using structural data from ref. 36) in the temperature range of 300–650 K, where no appreciable chemical expansion due to oxygen loss is observed. Therefore the presence of HS-Co^{3+} in the crystal structure of $Sr_2Co_{1.2}Ga_{0.8}O_5$ helps us to avoid temperature induced LS–HS transition and resulted in substantial decrease of TEC.

To assess the orbital energies in the axially distorted CoO_6 octahedra, we performed band-structure calculations for ordered structural models. The crystal structure of $Sr_2Co_{1.2}Ga_{0.8}O_5$ entails two types of disorders: (i) random positions of the O3 atoms on the 8i site with half occupancy (disordered arrangement of the tetrahedral chains); and (ii) mixing of Co and Ga on the tetrahedral and octahedral sites. Regarding the O3 atoms, we used different ordered structures with lower symmetries and found that the ordering of the O3

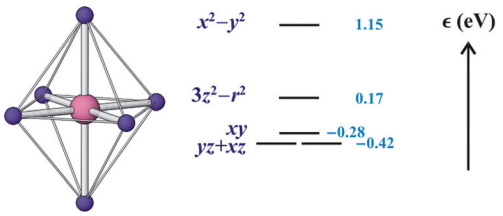

Fig. 4 Orbital energies (in eV) for $Sr_2Co_{1.2}Ga_{0.8}O_5$. The Fermi level is at zero energy.

atoms has little influence on the orbital energies at the octahedral site. Regarding the Co/Ga disorder, both "$Sr_2Co_2O_5$" (Co^{3+} in both octahedral and tetrahedral positions) and "Sr_2CoGaO_5" (Co^{3+} in the octahedra, Ga^{3+} in the tetrahedra) models were considered and they produced very similar orbital energies that differed by less than 0.01 eV.

The one-electron orbital levels in $Sr_2Co_{1.2}Ga_{0.8}O_5$ are shown in Fig. 4. The axial distortion has moderate influence on the t_{2g} levels (*xy*, *yz*, *xz*) that are split by about 0.14 eV, with the *xy* level lying higher in energy. On the other hand, the two e_g levels are split by nearly 1 eV, with the $3z^2 - r^2$ orbital being substantially more favourable than its $x^2 - y^2$ counterpart. These results follow the anticipated crystal-field picture that assumes lower energies for the *yz*, *xz* and $3z^2 - r^2$ orbitals because of the increased Co–O distances along *z*.

To probe directly the valence and spin states of the Co ions in $Sr_2Co_{1.2}Ga_{0.8}O_5$, we performed XAS measurements at the Co-$L_{2,3}$ edge. The Co (2p→3d) transitions at the Co-$L_{2,3}$ edges involve directly the relevant valence shell and are extremely sensitive to the charge and spin states.[1,2,5,37]

Fig. 5 shows the experimental Co-$L_{2,3}$ XAS spectrum of (d) $Sr_2Co_{1.2}Ga_{0.8}O_5$ (black line) together with (a) CoO, (b) $EuCoO_3$ and (c) Sr_2CoO_3Cl (magenta line) as references for HS-Co^{2+}, LS-Co^{3+}, and HS-Co^{3+}, respectively. The Co spectra of different valences show distinct multiplet structures at different absolute energies. While the main peak for CoO lies at around 779 eV, the main peak for both Co^{3+} compounds lies at 780.6 eV. This is consistent with the generally accepted notion that the increase in the valence state (from Co^{2+} to Co^{3+}, for example) typically results in the shift of the $L_{2,3}$ XAS spectra to higher energies by 1 eV or more.[5,37] Also note that the lowest energy peak at 777.8 eV is characteristic for octahedrally coordinated Co^{2+} as it lies well below in energy than any features of Co^{3+} or Co^{4+}.[38]

From Fig. 5 one can see that the $Sr_2Co_{1.2}Ga_{0.8}O_5$ spectrum lies at the same energy as both HS- and LS-Co^{3+} reference spectra and shows no spectral structure at 777.8 eV (feature *A*), indicating the absence of Co^{2+} ions. Therefore, the Co-$L_{2,3}$ XAS results establish that all Co ions are in a trivalent state in $Sr_2Co_{1.2}Ga_{0.8}O_5$. Moreover, oxides with the different spin states of Co^{3+} show different spectral structures, as follows: (1) at the Co-L_3 edge, the LS-$EuCoO_3$ spectrum has the pronounced higher energy shoulder *D* above the main peak *C* (Fig. 5), whereas the HS-Sr_2CoO_3Cl spectrum has the lower energy shoulder *B* below the main peak *C* at 780.6 eV. (2) At the L_2 edge, the LS-$EuCoO_3$ spectrum has a rather sharp main peak *E* at 795 eV with a high-energy shoulder, while the HS-Sr_2CoO_3Cl spectrum shows a weak main peak. (3) The HS-Co^{3+} in Sr_2CoO_3Cl shows a large *I*(L3)/*I*(L2) branching ratio as compared with the LS-Co^{3+} in $EuCoO_3$.

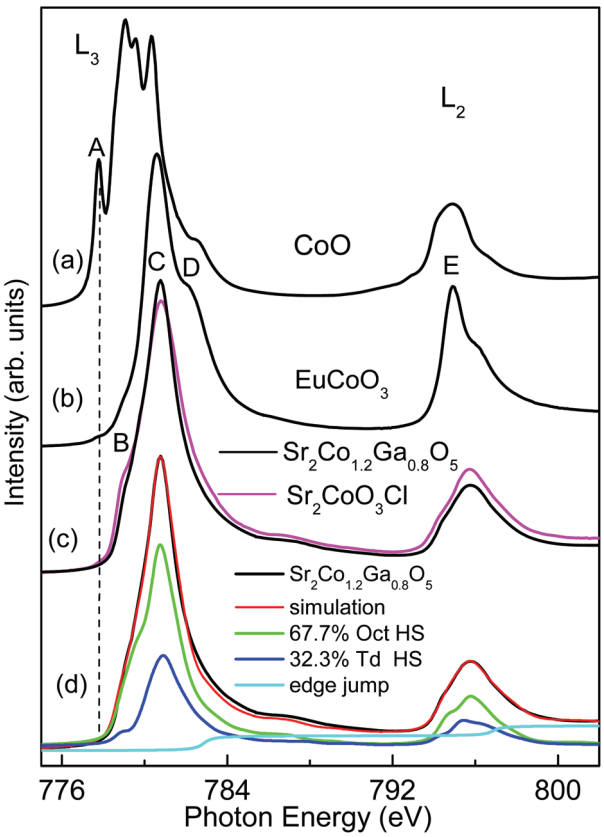

Fig. 5 Co $L_{2,3}$ edge spectra of references are (a) CoO (Co^{2+}), (b) $EuCoO_3$ (Co^{3+} LS, from ref. 2), and (c) Sr_2CoO_3Cl (Co^{3+} HS magenta line, from ref. 2), $Sr_2Co_{1.2}Ga_{0.8}O_5$ (black line) and curve (d) shows the experimental spectrum (black line) of $Sr_2Co_{1.2}Ga_{0.8}O_5$ in comparison with the simulation with HS Co^{3+} (red line).

Focusing now on the $Sr_2Co_{1.2}Ga_{0.8}O_5$ spectrum, one can clearly observe the low-energy shoulder below the main peak at the Co-L_3 edge and no sharp peak *E* at the Co-L_2 edge. Overall spectral features are very similar to those of HS-Sr_2CoO_3Cl, thus strongly hinting towards the HS-Co^{3+} state. However, the main peak (low energy shoulder) at the Co-L_3 edge in the $Sr_2Co_{1.2}Ga_{0.8}O_5$ spectrum has a slightly larger (lower) spectral weight than that in the Sr_2CoO_3Cl spectrum. To understand this difference, we have simulated the experimental $Sr_2Co_{1.2}Ga_{0.8}O_5$ spectrum using the configuration–interaction cluster model that includes the full atomic multiplet theory and the hybridization with the O 2p ligands.[39] For this we use parameter values typical for HS-Co^{3+} in octahedral[1] and tetrahedral coordinations.[7] The Co 3d to O 2p transfer integrals were adapted for the Co–O bond lengths according to Harrison's description.[40] The model calculations were done using the XTLS 9.0 code.[39,41] In the analysis, we considered the amounts of Co^{3+} in the octahedral and tetrahedral

positions of the brownmillerite structure as calculated from the results of the NPD data refinement. It follows that 32.3% of the total amount of Co^{3+} is located in tetrahedral and 67.7% in octahedral sites of the crystal structure. One can observe from Fig. 5(d) that all experimental (black line) spectral structures at both the Co-L_2 and Co-L_3 edges were well reproduced by the theoretical simulation (red line) with a ratio of 32.3% Co_{Td}^{3+} (blue line) and 67.7% Co_{Oct}^{3+} (green line), both in the HS state. The slightly larger spectral weight of the main peak in $Sr_2Co_{1.2}Ga_{0.8}O_5$, as compared with that in Sr_2CoO_3Cl, is attributed to the 32.3% tetrahedral HS-Co^{3+} ions in the former. Tetrahedral HS-Co^{3+} ions display a very weak lower energy shoulder below the L_3 main peak.[7]

Therefore, both low-temperature NPD and XAS studies show the presence of Co^{3+} in the HS ground state at both octahedral and tetrahedral sites in the $Sr_2Co_{1.2}Ga_{0.8}O_5$ brownmillerite. Stabilization of the HS-Co^{3+} in octahedra seems to have resulted from long Co–O distances in the crystal structure, which in turn occurs due to the presence of large A-cation like Sr^{2+}. However, the HS state observed in $Sr_2Co_{1.2}Ga_{0.8}O_5$ is not a trivial result considering the large tetragonal distortion of the CoO_6 octahedron, as confirmed by the structure refinement at 2 K (1.9591(4) Å for Co–O_{eq} and 2.257(6) Å for Co–O_{ax}). In this case, one would anticipate the formation of the IS state.[9,10,16] For example, in $LaCoO_3$ with its LS state of Co^{3+} at low temperatures, d(Co–O) at 5 K is 1.925 Å and approaching 1.962 Å only at 1000 K.[36] The octahedral distortion in $Sr_2Co_{1.2}Ga_{0.8}O_5$ defined as the difference between the axial and equatorial bond lengths normalized by their average is 0.14. This value is much larger in comparison with ~0.06 reported in ref. 16 for $LaCoO_3$, where the presence of IS-Co^{3+} is claimed. It should be mentioned that in $Sr_3YCo_4O_{10.76}$ with a layered structure and a similar octahedral distortion of 0.062 (1.913(3) Å for Co–O_{eq} and 2.035(6) Å for Co–O_{ax} at 14 K), the refined magnetic moment of octahedrally coordinated cobalt ions (~1.2μ_B at 14 K) indicates the mixture of HS- and LS-Co^{3+}.[42]

The distortions of the CoO_6 octahedra can also be considered from the microscopic perspective. To this end, we compare the orbital energies in $Sr_2Co_{1.2}Ga_{0.8}O_5$ to those in $LaCoO_3$. The trigonal distortion in the latter compound imposes a weak splitting of the three t_{2g} levels into the a_{1g} singlet and e_g' doublet. The effective octahedral crystal-field splitting Δ_o calculated as the energy difference between the e_g levels and the center of gravity of a_{1g} and e_g' is 1.45 eV. In contrast, we find the much lower Δ_o = 1.03 eV in $Sr_2Co_{1.2}Ga_{0.8}O_5$. This difference can also be seen as a large reduction in the $3z^2 - r^2$ energy with a very little change in the $x^2 - y^2$ energy upon the axial elongation of the CoO_6 octahedron. The IS-Co^{3+} requires that no electrons occupy the $x^2 - y^2$ state, but the energy of this state is probably not high enough to render it energetically unfavourable. Altogether, orbital energies of Co^{3+} in the axially elongated CoO_6 octahedra are such that the HS-Co^{3+} is formed instead of IS-Co^{3+}, and even the combination of the LS- and HS-states, as proposed for $LaSrCoO_4$,[4] turns out to be more favourable than the IS-Co^{3+} state. The stabilization of the IS state requires that not only the energy of the $3z^2 - r^2$ orbital is reduced, but also the energy of the $x^2 - y^2$ orbital is increased substantially. However, this may be difficult to achieve in real crystals because of the bond valences and other crystallo-chemical constrains.

Conclusions

In conclusion, the NPD study of the brownmillerite-like cobaltate $Sr_2Co_{1.2}Ga_{0.8}O_5$ at 2 K shows large interatomic distances in the highly distorted CoO_6 octahedron with 1.9591(4) Å and 2.257(6) Å for equatorial and axial Co–O bonds, respectively. Together with the value of 3.82(7)μ_B for the refined magnetic moment of Co^{3+} at the octahedral site, this indicates the presence of HS-Co^{3+}. The detailed analysis of the spectral structures in the soft XAS study of $Sr_2Co_{1.2}Ga_{0.8}O_5$ at the both Co-L_2 and Co-L_3 edges unambiguously shows that the large tetragonal distortion of the CoO_6 octahedron does not stabilize an IS-Co^{3+} state as often suggested, but rather keeps the Co^{3+} ions in the HS state. The presence of large A-cations in perovskite-like oxides resulted in large Co–O interatomic distances and may lead to the suppression of the LS ground state of Co^{3+} and results in drastically decreased TEC. This can help in the design of cobalt-based cathode materials for SOFC with TEC close to solid electrolytes like YSZ and GDC.

Acknowledgements

This work was supported by the Russian Science Foundation (grant no. 14-13-00680), the Skolkovo Institute of Science and Technology (Center of Electrochemical Energy) and the MSU-development Program up to 2020. A.T. acknowledges the funding from ESF through the Mobilitas MTT77 grant.

Notes and references

1 M. W. Haverkort, Z. Hu, J. C. Cezar, T. Burnus, H. Hartmann, M. Reuther, C. Zobel, T. Lorenz, A. Tanaka, N. B. Brookes, H. H. Hsieh, H.-J. Lin, C. T. Chen and L. H. Tjeng, *Phys. Rev. Lett.*, 2006, **97**, 176405.
2 Z. Hu, H. Wu, M. W. Haverkort, H. H. Hsieh, H.-J. Lin, T. Lorenz, J. Baier, A. Reichl, I. Bonn, C. Felser, A. Tanaka, C. T. Chen and L. H. Tjeng, *Phys. Rev. Lett.*, 2004, **92**, 207402.
3 J. Wang, W. Zhang and D. Y. Xing, *Phys. Rev. B: Condens. Matter*, 2000, **62**, 14140.
4 H. Wu, *Phys. Rev. B: Condens. Matter*, 2010, **81**, 115127.
5 T. Burnus, Z. Hu, M. W. Haverkort, J. C. Cezar, D. Flahaut, V. Hardy, A. Maignan, N. B. Brookes, A. Tanaka, H. H. Hsieh, H.-J. Lin, C. T. Chen and L. H. Tjeng, *Phys. Rev. B: Condens. Matter*, 2006, **74**, 245111.
6 M. García-Fernández, V. Scagnoli, U. Staub, A. M. Mulders, M. Janousch, Y. Bodenthin, D. Meister, B. D. Patterson, A. Mirone, Y. Tanaka, T. Nakamura, S. Grenier, Y. Huang

and K. Conder, *Phys. Rev. B: Condens. Matter*, 2008, **78**, 054424.
7 N. Hollmann, Z. Hu, M. Valldor, A. Maignan, A. Tanaka, H. H. Hsieh, H.-J. Lin, C. T. Chen and L. H. Tjeng, *Phys. Rev. B: Condens. Matter*, 2009, **80**, 085111.
8 A. Maignan, V. Caignaert, B. Raveau, D. Khomskii and G. Sawatzky, *Phys. Rev. Lett.*, 2004, **93**, 026401.
9 A. A. Taskin and Y. Ando, *Phys. Rev. Lett.*, 2005, **95**, 176603.
10 W. Kobayashi, S. Yoshida and I. Terasaki, *J. Phys. Soc. Jpn.*, 2006, **75**, 103702.
11 Y. Zhang, S. Sasaki and M. Izumi, *Phys. Status Solidi B*, 2007, **244**, 4550–4553.
12 S. Tsubouchi, T. Kyomen, M. Itoh, P. Ganguly, M. Oguni, Y. Shimojo, Y. Morii and Y. Ishii, *Phys. Rev. B: Condens. Matter*, 2002, **66**, 052418.
13 C. Bernhard, A. V. Boris, N. N. Kovaleva, G. Khaliullin, A. V. Pimenov, L. Yu, D. P. Chen, C. T. Lin and B. Keimer, *Phys. Rev. Lett.*, 2004, **93**, 167003.
14 M. Daghofer, P. Horsch and G. Khaliullin, *Phys. Rev. Lett.*, 2006, **96**, 216404.
15 J. Chaloupka and G. Khaliullin, *Phys. Rev. Lett.*, 2007, **99**, 256406.
16 G. Maris, Y. Ren, V. Volotchaev, C. Zobel, T. Lorenz and T. T. M. Palstra, *Phys. Rev. B: Condens. Matter*, 2003, **67**, 224423.
17 P. M. Raccah and J. B. Goodenough, *Phys. Rev.*, 1967, **155**, 932–943.
18 A. Petric, P. Huang and F. Tietz, *Solid State Ionics*, 2000, **135**, 719–725.
19 S. Uhlenbruck and F. Tietz, *Mater. Sci. Eng., B*, 2004, **107**, 277–282.
20 S. Shafeie, J. Grins, S. Istomin, A. A. Gippius, L. Karvonen, S. Populoh, A. Weidenkaff, J. Koehler and G. Svensson, *J. Mater. Chem.*, 2012, **22**, 16269–16276.
21 A. A. Colville and S. Geller, *Acta Crystallogr., Sect. B: Struct. Crystallogr. Cryst. Chem.*, 1971, **27**, 2311–2315.
22 J. C. Grenier, S. Ghodbane, G. Demazeau, M. Pouchard and P. Hagenmuller, *Mater. Res. Bull.*, 1979, **14**, 831–839.
23 J. Rodriguez, J. M. Gonzalez-Calbet, J. C. Grenier, J. Pannetler and M. Anne, *Solid State Commun.*, 1987, **62**, 231–234.
24 A. Muñoz, C. de la Calle, J. A. Alonso, P. M. Botta, V. Pardo, D. Baldomir and J. Rivas, *Phys. Rev. B: Condens. Matter*, 2008, **78**, 054404.
25 E. Sullivan, J. Hadermann and C. Greaves, *J. Solid State Chem.*, 2011, **184**, 649–654.
26 C. de la Calle, A. Aguadero, J. A. Alonso and M. T. Fernandez-Dıaz, *Solid State Sci.*, 2008, **10**, 1924–1935.
27 F. Lindberg, S. Y. Istomin, P. Berastegui, G. Svensson, S. M. Kazakov and E. V. Antipov, *J. Solid State Chem.*, 2003, **173**, 395–406.
28 F. Lindberg, G. Svensson, S. Ya. Istomin, S. V. Aleshinskaya and E. V. Antipov, *J. Solid State Chem.*, 2004, **177**, 1592–1597.
29 S. Ya. Istomin, S. V. Abdyusheva, G. Svensson and E. V. Antipov, *J. Solid State Chem.*, 2004, **177**, 4251–4257.
30 S. Lambert, H. Leligny, D. Grebille, D. Pelloquin and B. Raveau, *Chem. Mater.*, 2002, **14**, 1818–1826.
31 C. Mitra, R. S. Fishman, S. Okamoto, H. N. Lee and F. A. Reboredo, *J. Phys.: Condens. Matter*, 2014, **26**, 036004.
32 K. Luo and M. A. Hayward, *Dalton Trans.*, 2014, **43**, 1571–1576.
33 A. C. Larson and R. B. Von Dreele, General Structure Analysis System (GSAS), Los Alamos National Laboratory Report LA-UR-86-748, 2000; B. H. Toby, EXPGUI, a graphical user interface for GSAS, *J. Appl. Crystallogr.*, 2001, **34**, 210.
34 K. Koepernik and H. Eschrig, *Phys. Rev. B: Condens. Matter*, 1999, **59**, 1743.
35 J. P. Perdew and Y. Wang, *Phys. Rev. B: Condens. Matter*, 1992, **45**, 13244.
36 P. G. Radaelli and S.-W. Cheong, *Phys. Rev. B: Condens. Matter*, 2002, **66**, 094408.
37 C. F. Chang, Z. Hu, H. Wu, T. Burnus, N. Hollmann, M. Benomar, T. Lorenz, A. Tanaka, H.-J. Lin, H. H. Hsieh, C. T. Chen and L. H. Tjeng, *Phys. Rev. Lett.*, 2009, **102**, 116401.
38 H.-J. Lin, Y. Y. Chin, Z. Hu, G. J. Shu, F. C. Chou, H. Ohta, K. Yoshimura, S. Hébert, A. Maignan, A. Tanaka, L. H. Tjeng and C. T. Chen, *Phys. Rev. B: Condens. Matter*, 2010, **81**, 115138.
39 A. Tanaka and T. Jo, *J. Phys. Soc. Jpn.*, 1994, **63**, 2788.
40 W. A. Harrison, *Electronic Structure and the Properties of Solids*, Dover, New York, 1989.
41 Parameters [eV]: U_{dd} = 5.5, U_{cd} = 7.0, Δ = 2. For the tetrahedral sites, the 10 Dq = −0.2. For the octahedral sites 10 Dq = 0.75, Δe_g = 0.6, Δt_{2g} = 0.03, effectively 1.04, 0.98, and 0.14, respectively.
42 D. V. Sheptyakov, V. Yu. Pomjakushin, O. A. Drozhzhin, S. Ya. Istomin, E. V. Antipov, I. A. Bobrikov and A. M. Balagurov, *Phys. Rev. B: Condens. Matter*, 2009, **80**, 024409.